Supporting Information

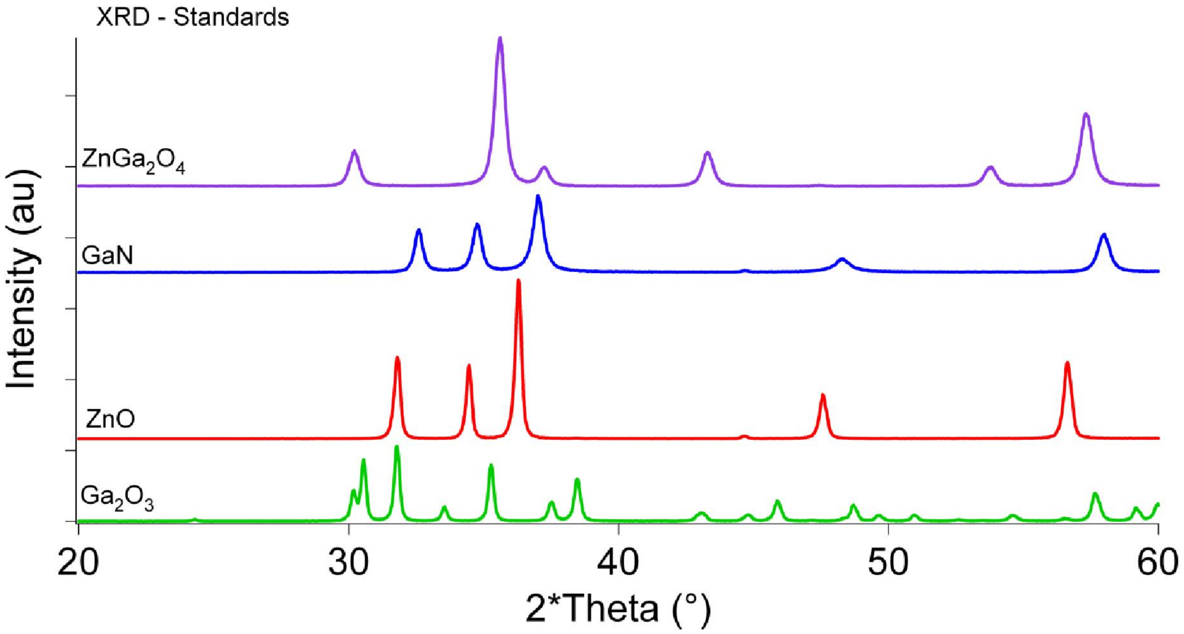

Figure S1. XRD patterns of $ZnGa_2O_4$, GaN, ZnO, and Ga_2O_3.

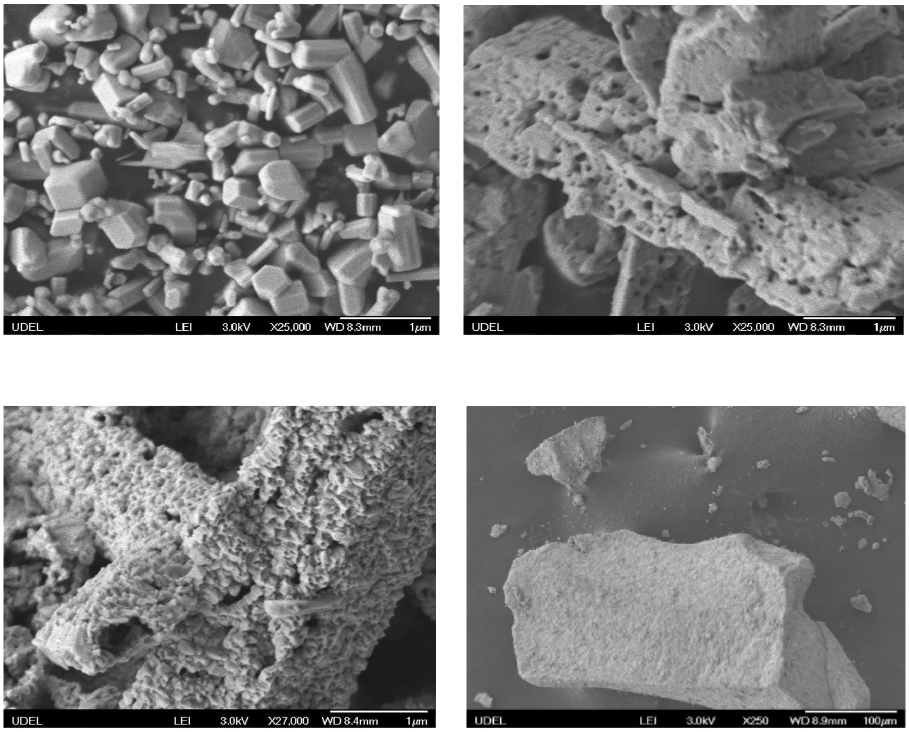

Figure S2. SEM micrographs for ZnO (A), Ga_2O_3 (B), GaN (C), $ZnGa_2O_4$ (D).

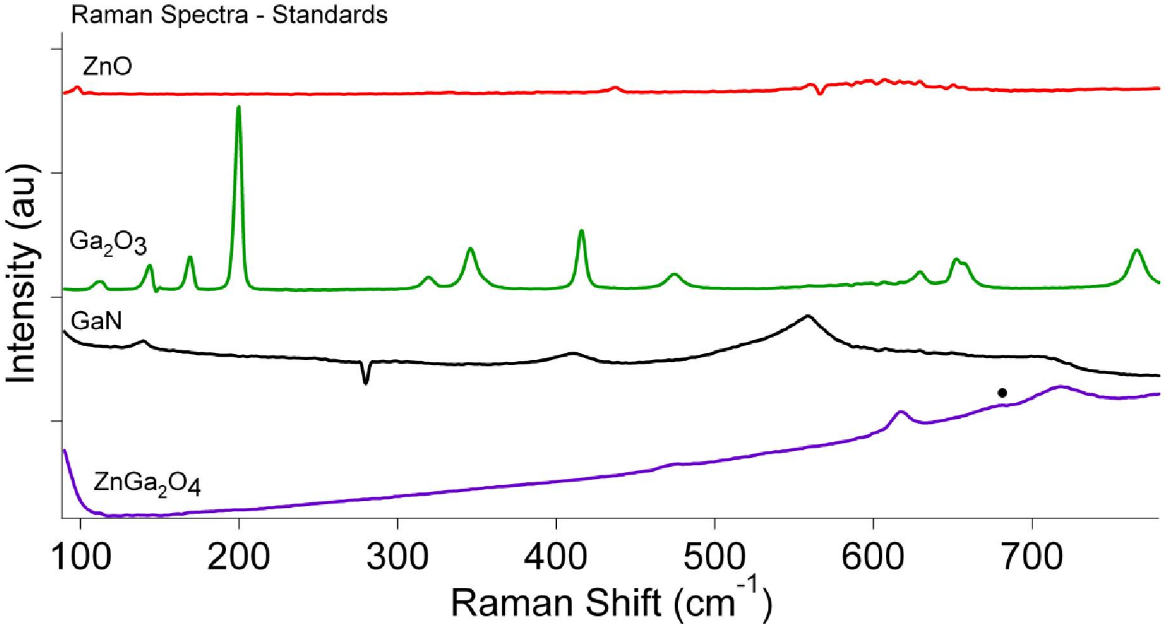

Figure S3A. Raman shifts associated with ZnO, Ga_2O_3, GaN and $ZnGa_2O_4$. • - represents the additional second order mode for the spinel. GaN and ZnO like other synthesized wurzites show broad and convoluted Raman bands which are attributed to poor long order and disorders. As can be seen in Table S3, these samples have poor long range order.

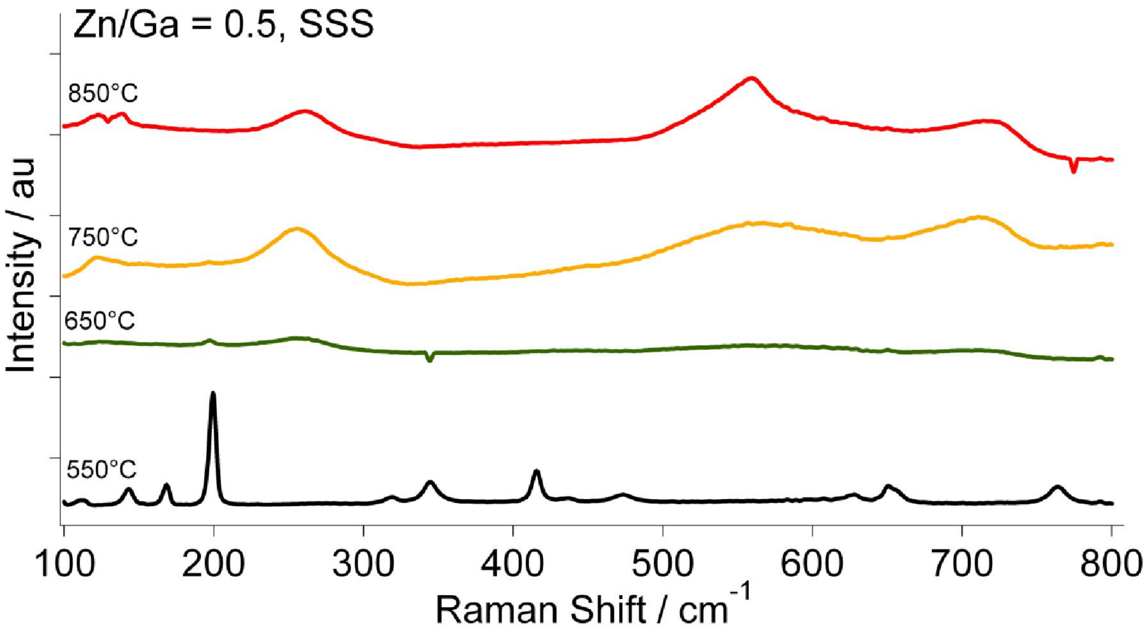

Figure S3B. Raman spectra of the products prepared at different nitridation temperatures; the starting material is the SSS precursor. Some of the sharp peaks that appear in the opposite direction are cosmic spikes.

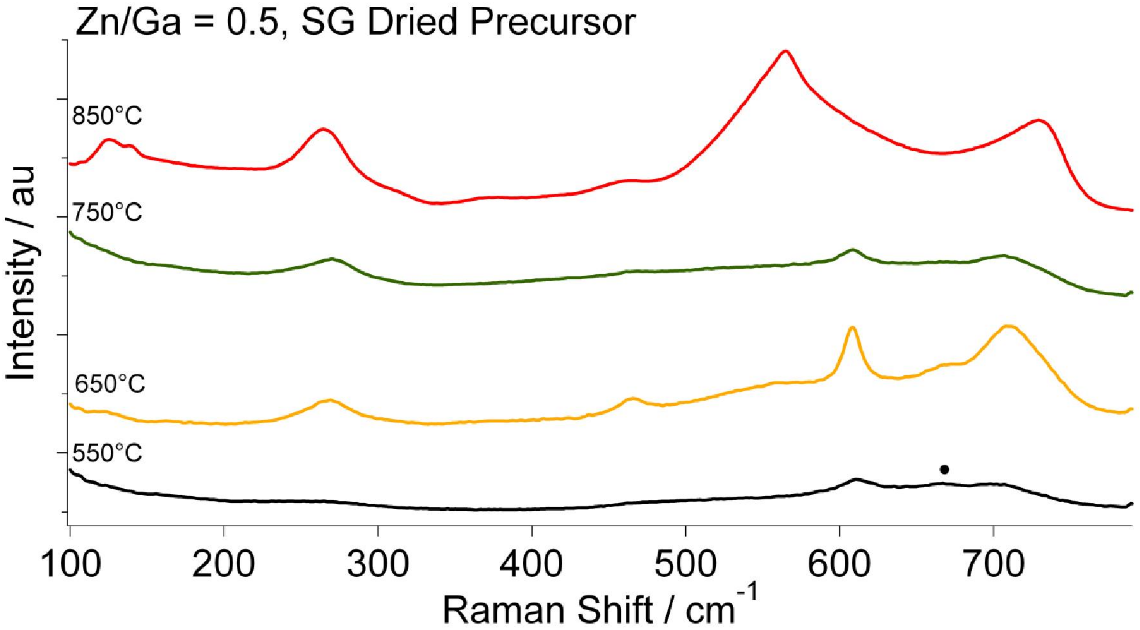

Figure S3C. Raman spectra of the products prepared at different nitridation temperatures; the starting material is the SG dried precursor. Some of the sharp peaks that appear in the opposite direction are cosmic spikes. • - represents the additional second order mode for the spinel.

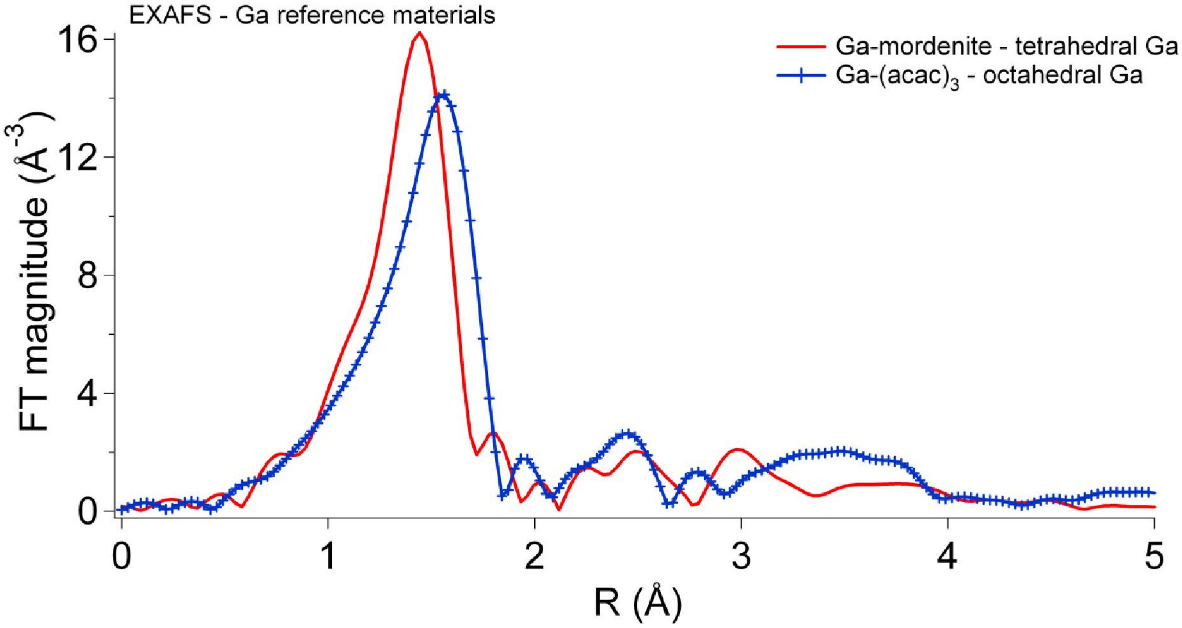

Figure S4A. The EXAFS spectra (Ga-K edge) of Tetrahedral Ga (Ga-Mordenite) and Octahedral Ga ($Ga(CH_3COCHCOCH_3)_3$) as reference materials (not phase corrected).

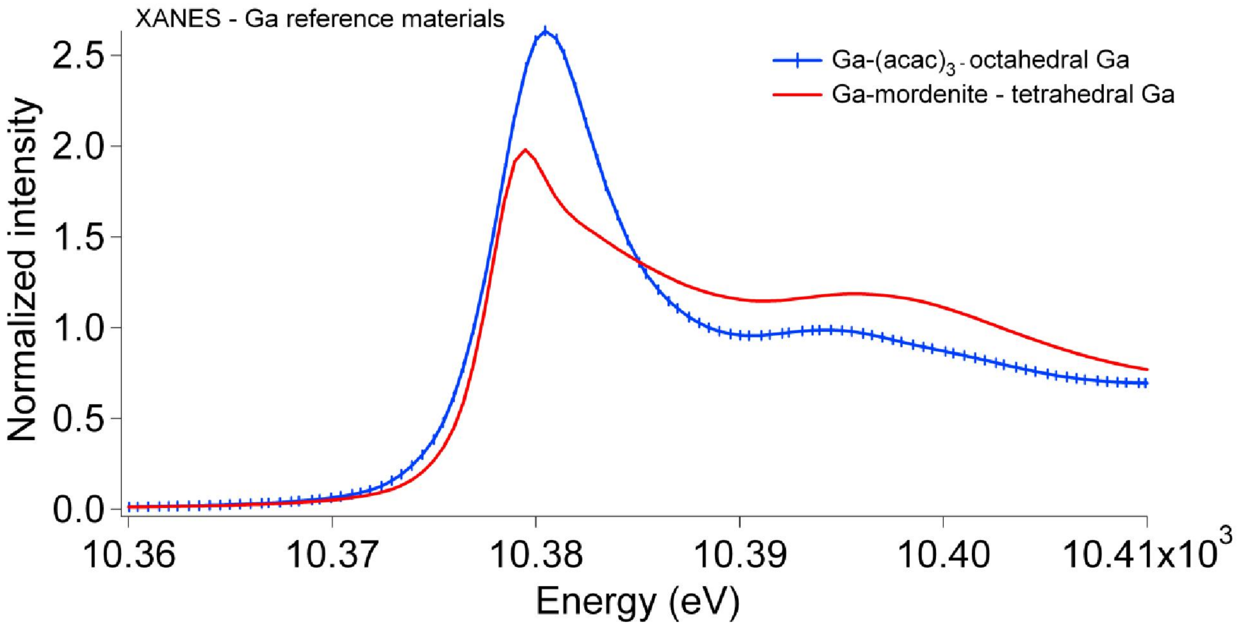

Figure S4B. The XANES spectra (Ga-K edge) of Tetrahedral Ga (Ga-Mordenite) and Octahedral Ga ($Ga(CH_3COCHCOCH_3)_3$) as reference materials.

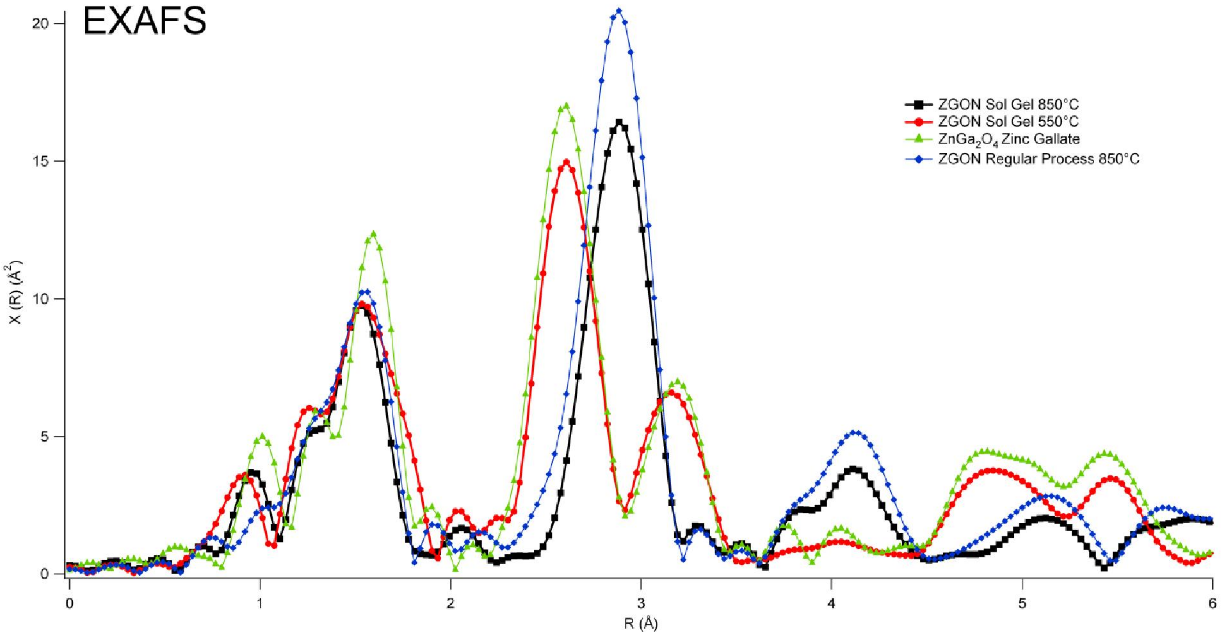

Figure S5. The EXAFS spectra (Ga-K edge) of the spinels and wurzites (not phase corrected). Here you can clearly see the decreased first and third shell Ga-(O/N) bond lengths of the nitrided spinel ZGON (with tetrahedral Ga centers, 550^{o}C) as compared to the spinel $ZnGa_2O_4$ oxide (octahedral Ga) and the wurzite ZGONs (tetrahedral Ga, 850^{o}C).

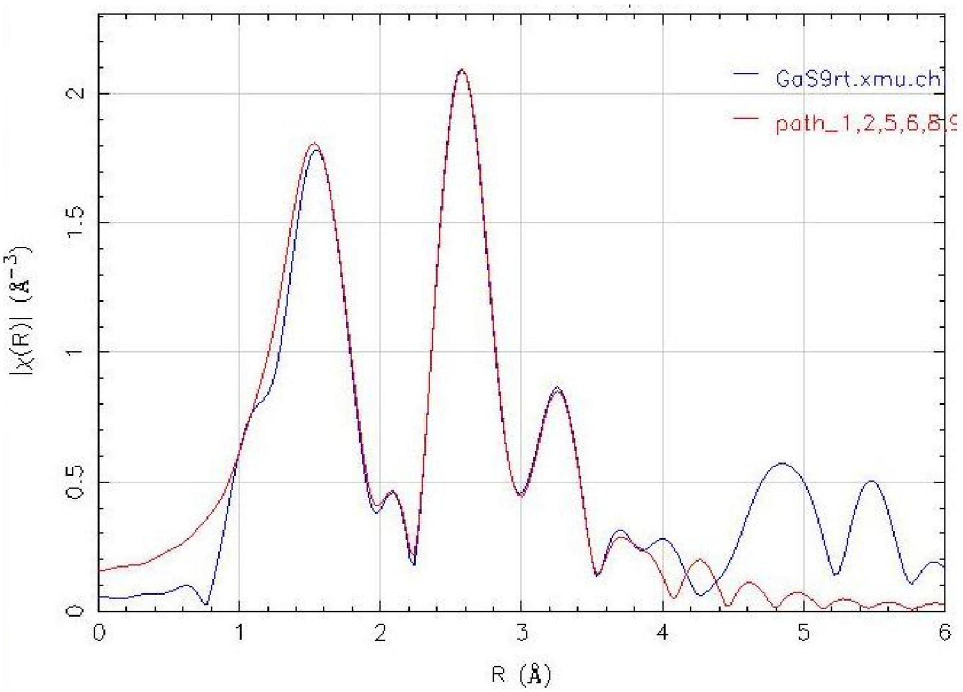

Figure S6A. Fourier transformed EXAFS data and the scattering fit (in red) for spinel zinc gallium oxide.

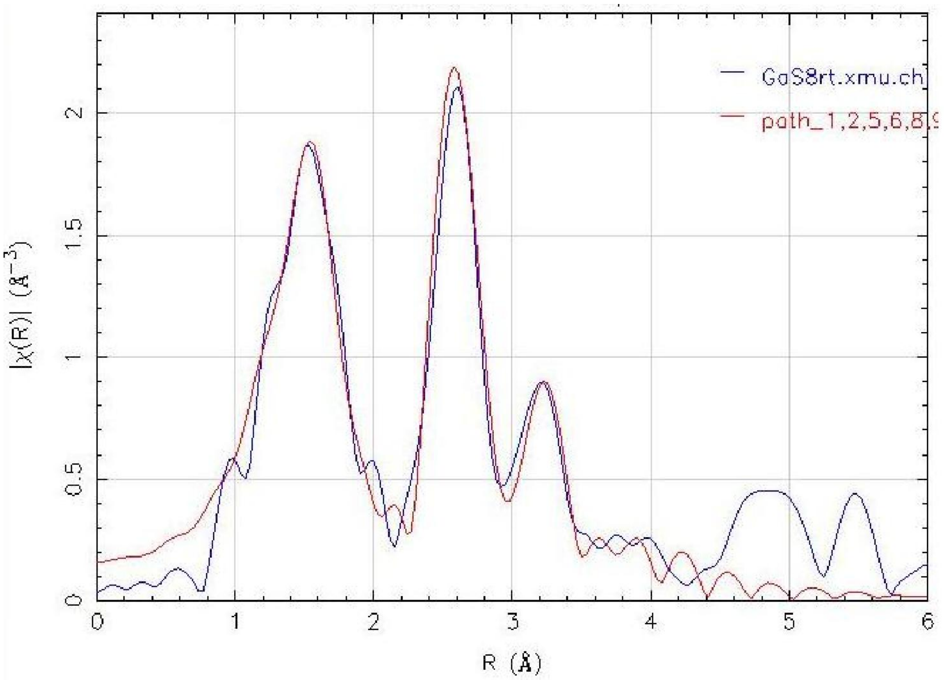

Figure S6B. Fourier transformed EXAFS data and the scattering fit (in red) for spinel zinc gallium oxynitride (SG 550°C).

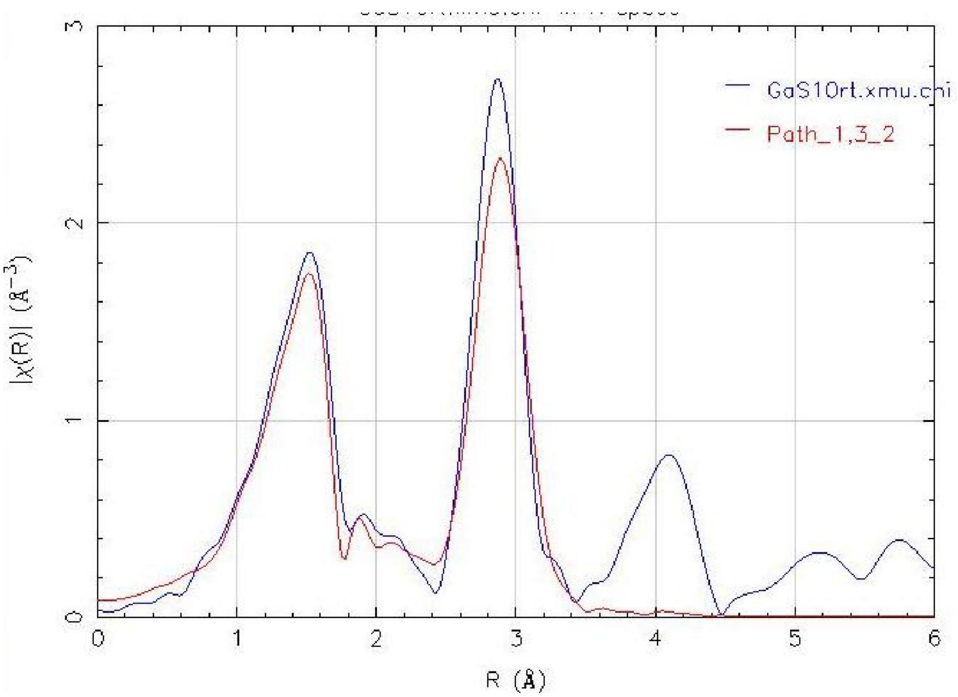

Figure S6C. Fourier transformed EXAFS data and the scattering fit (in red) for wurzite zinc gallium oxynitride (SSS 850°C).

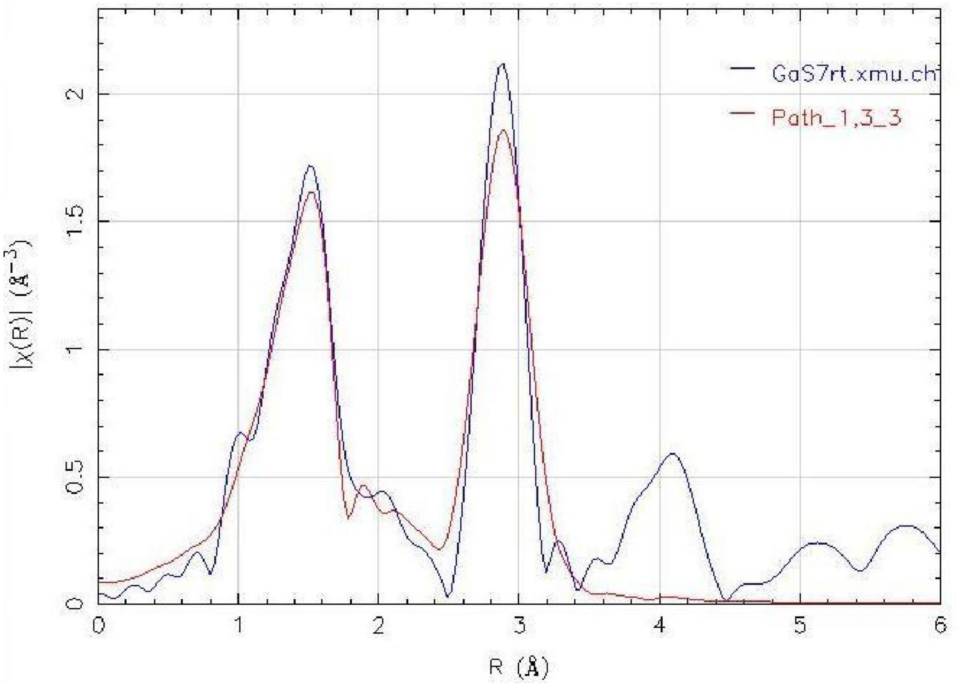

Figure S6D. Fourier transformed EXAFS data and the scattering fit (in red) for wurzite zinc gallium oxynitride (SG 850°C).

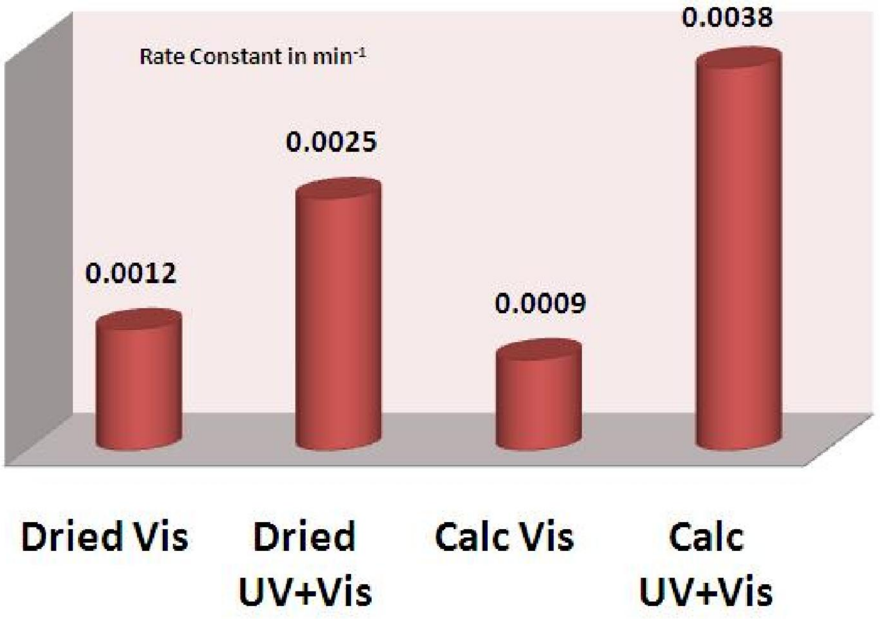

Figure S7. First order rate constant for the dye degradation reactions done using different spinel ZGON photocatalysts (dried and calcined).

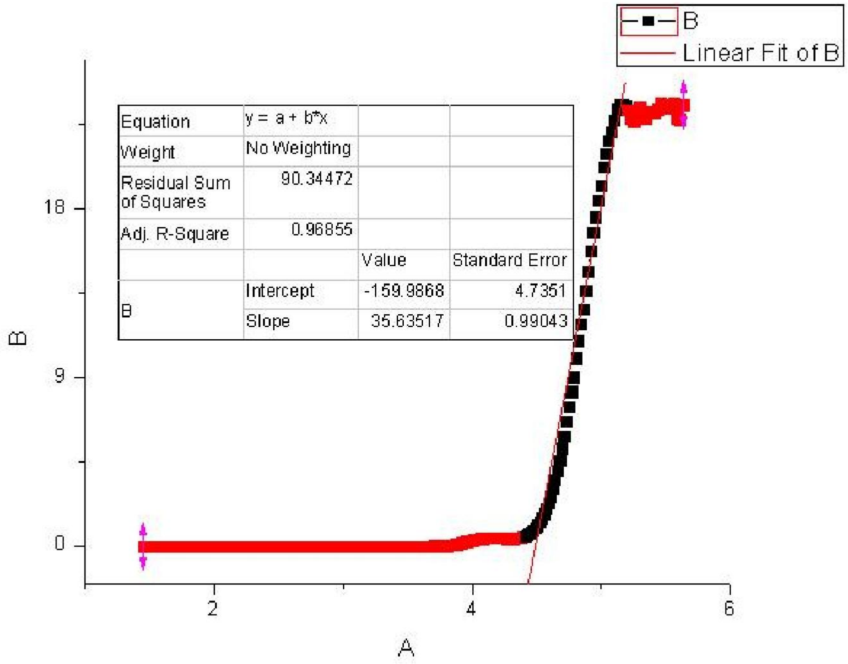

Figure S8. $[F(R_\infty)h\nu]^2$ vs $(h\nu)$ curves for sol-gel derived $ZnGa_2O_4$ precursor. The band gap is determined from a straight line fit for the linear region of the graph. Thus, the band gap of $ZnGa_2O_4$ is -(-159.99)/35.64 = 4.49 eV.

Experimental

The GaN sample that was used as a standard was obtained by nitriding Ga_2O_3 in ammonia at 850°C for 15 hours. Ga-mordenite was synthesized in solutions of molar composition 20 SiO_2 / 300 H_2O / 4 Na_2O / 1 Ga_2O_3. In the first step water, sodium hydroxide, and gallium oxide where mixed together and heated to 100°C for 1 day. To the resulting clear solution Ludox AS-40 was added to obtain a synthesis solution of the above molar composition. These final solutions were loaded into acid-digestion vessels (Parr) and then heated to 150°C for seven days while rotated at ~40 rpm. Gallium Acetylacetonate used for XAS measurements was obtained from Sigma-Aldrich.

Neutron Diffraction – Analysis of cation movement from octahedral to tetrahedral sites

Spinels can undergo a multitude of cationic distributions such that octahedrons and tetrahedrons are relaxed, we in the following section have studied the absence of oxygen vacancies and to balance the charge brought in by the nitrogen anions, we then proceeded to introduce Ga and Zn cations in the vacant tetrahedral positions.

The combination of both Zn and Ga interstitials (for N = 1.15%) was ruled out because of mismatch of neutron diffraction intensities (Figure S9A). This might be due to the huge energies required to form double cation vacancies and consequently move them to interstitial positions.

The other model which happens to approximately fit the neutron diffraction results (for N ~ 1.15%) is the presence of Ga^{3+} in other tetrahedral sites with Zn occupying interstitial tetrahedral positions. The presence of Zn interstitials has been predicted to have the lowest formation energies among all Frenkel defects possible.[1] For this refinement results refer Figure S9B and Table S1. Even here the refinements are not perfect and the oxygen vacancy model with gallium cation inversion described in the paper is plausible due to prior work done on Ga-O-N spinels which are similar to ours and show the same oxygen and octahedral gallium deficiencies. The EXAFS results also indicate the presence of tetrahedral Ga centers which were also observed in the neutron refinements.

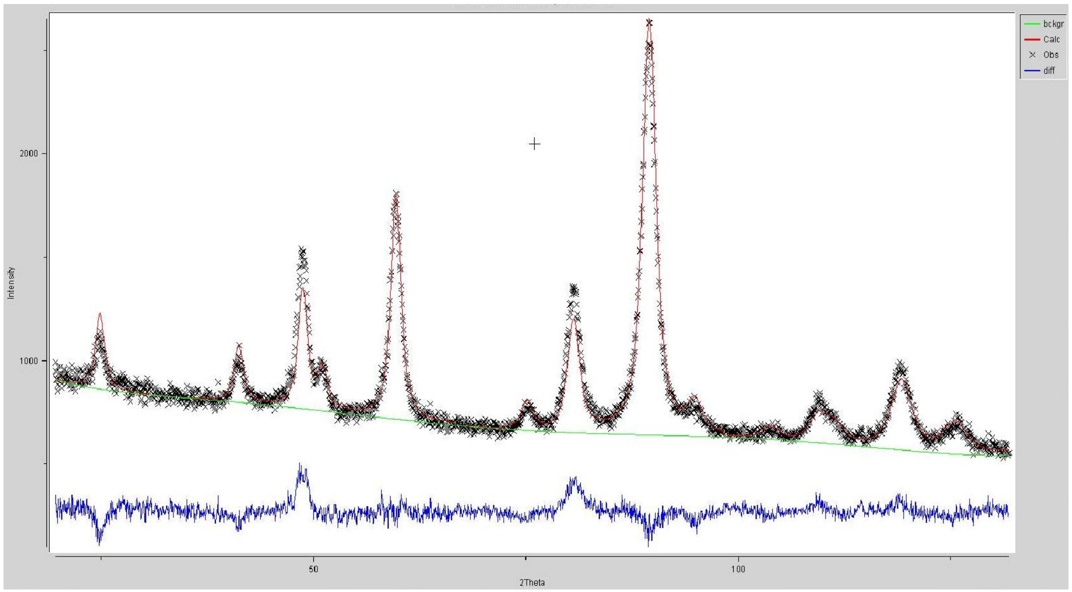

Figure S9A. Neutron diffraction refinement involving a fraction of both cations in interstitial positions for N~1.15%.

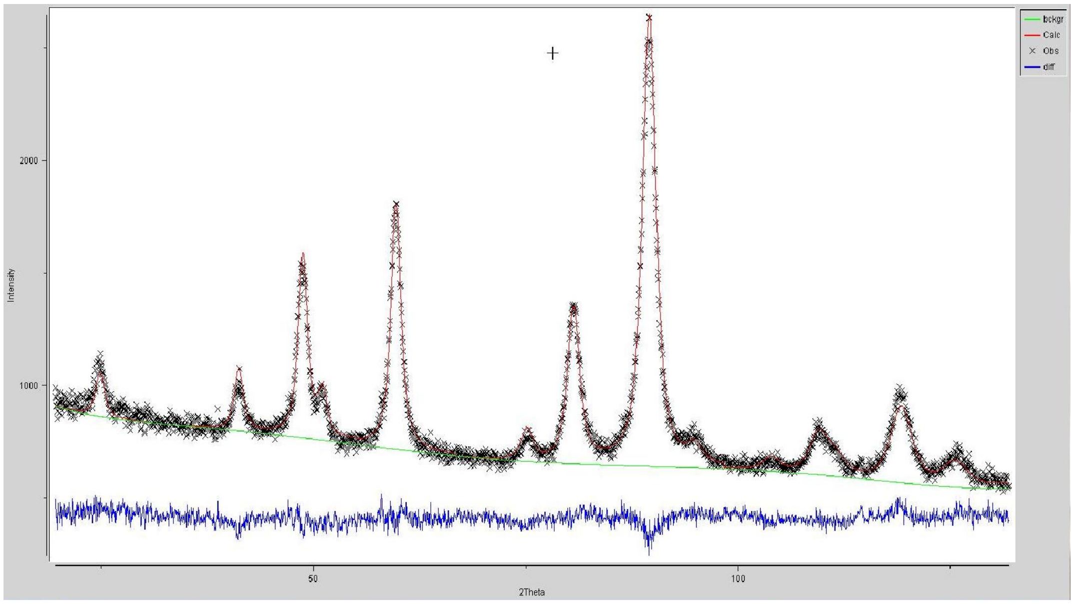

Figure S9B. Neutron diffraction refinement involving a fraction of Zn tetrahedral interstitials with Ga in other tetrahedral positions for N~1.15%.

Table S1. Results from the Rietveld refinement of neutron diffraction data of the spinel oxy-nitride involving both Ga and Zn in tetrahedral positions with no anion vacancies (corresponding to Figure S8B).

Atom	Position	x	y	z	Occupancy	U_{iso}
Zn	Regular Tetrahedral	0.125	0.125	0.125	0.9441	0.005
Zn*	Interstitial Tetrahedral*	0.125	0.625	0.125	0.0838	0.005
Ga	Regular Octahedral	0.5	0.5	0.5	0.9441	0.005
Ga	Regular Tetrahedral	0.875	0.375	0.375	0.1677	0.005
O		0.2591	0.2591	0.2591	0.9441	0.005
N		0.2591	0.2591	0.2591	0.0559	0.005

The refinement is a continuation of the spinel crystal system from the refined oxy-nitride (Table 4). The unit cell parameter is 8.3398 Å, molecular weight = 266.617 units. The parameters of fit are**,** $_wR_p$ (Fit – Bknd) = 3.16%, R_p (Fit – Bknd) = 2.76%. N wt% = 1.15. Atomic Zn/Ga = 2. * - Zn could also occupy the other interstitial position x=y=z=0.375 and this does not affect the refinement results.

Table S2. Refined crystal parameters for the spinel zinc gallium oxide precursor synthesized using the sol-gel procedure.

	Zinc Gallate		
Formula	$ZnGa_2O_4$		
Crystal System	Cubic Spinel		
Space Group	$Fd\bar{3}m$		
a=b=c (Å)	8.3376(1)		
α=β=γ	90°		
Elements	Zn	Ga	O
Atomic Positions (x=y=z)	0.125	0.5	0.2608(1)
Atomic Occupancies	1	1	1
Displacement Parameter (Å^2)	0.005	0.005	0.005
Agreement Factors, $_wR_p$ (Fit – Bknd)	2.84%		
R_p (Fit-Bknd)	2.59%		
Final Σ(Shift/esd)^2	0.0071		

Table S3. Comparison between the coherence length and the average particle size of the spinel and wurzite ZGONs

Sample	**Coherence Length XRD**[1] **nm**	**Average Particle Size**[2] **nm**	***"Crystallinity"*** **Coh. lt./Ave. part. size**
SSS 750°C Wurzite[3]	27	279	0.096
SSS 850°C Wurzite[3]	40	443	0.09
SG dried 850°C Wurzite[3]	33	199	0.166
SG calcined 850°C Wurzite[3]	16	70	0.23
SG dried 550°C Spinel[4]	9.5	27	0.352
SG calcined 550°C Spinel[4]	21	62	0.34
ZnO	45	88	0.511
GaN	23.6	195	0.118

[1] – From XRD measurements, average value using diffraction planes between 30 and 60° 2Θ. [2] – Average particle size was calculated using the spherical approximation, d = 6/(density in g/cm^3*surface area in cm^2/g). [3] – The density used was that of GaN 6.15 g/cm^3. [4] – The density used was that of the $ZnGa_2O_4$ structure from the neutron diffraction refinement ~ 6.06 g/cm^3.

The assumption of a spherical particle is a reasonable simplification and the table clearly indicates a big difference in the coherence length and the particle size which explains the absence of a long range order in our crystals leading to broadness of our Raman data. The assumption of a spherical particle is the lowest limit for particle size calculations. For a sphere the longest crystallite could only be the diameter whereas for a cube the largest crystallite is not the side but the longest diagonal. Thus any other approximation would give a higher ratio than what is calculated with a spherical approximation and presented in column 4.

1. P. Ravindra, D. G. Julian, K. S. Suresh and M. R. Jose, *J. Am. Ceram. Soc.*, 1999, **82**, 3337-3341.